ECS Journal of Solid State
Science and Technology

The Electrochemical Society
Advancing solid state & electrochemical science & technology

Light Extraction Efficiency Optimization of AlGaN-Based Deep-Ultraviolet Light-Emitting Diodes

To cite this article: Hui Wan *et al* 2020 *ECS J. Solid State Sci. Technol.* **9** 046002

View the article online for updates and enhancements.

This content was downloaded from IP address 159.226.165.18 on 28/04/2021 at 02:58

ECS Journal of Solid State Science and Technology, 2020 **9** 046002
2162-8777/2020/9(4)/046002/5/$40.00 © 2020 The Electrochemical Society ("ECS"). Published on behalf of ECS by IOP Publishing Limited

Light Extraction Efficiency Optimization of AlGaN-Based Deep-Ultraviolet Light-Emitting Diodes

Hui Wan,[1] Shengjun Zhou,[1,2,3,z] Shuyu Lan,[2] and Chengqun Gui[1]

[1]*The Institute of Technological Sciences, Wuhan University, Wuhan 430072, People's Republic of China*
[2]*Center for Photonics and Semiconductors, School of Power and Mechanical Engineering, Wuhan University, Wuhan 430072, People's Republic of China*
[3]*State Key Laboratory of Applied Optics, Changchun Institute of Optics, Fine Mechanics and Physics, Chinese Academy of Sciences, Changchun 130033, People's Republic of China*

Using finite-difference time-domain method, the light extraction efficiency (LEE) of AlGaN-based deep-ultraviolet light-emitting diodes (DUV LEDs) is investigated. Simulation results show that compared to flat sapphire substrate, the nano-patterned sapphire substrate (NPSS) expands the extraction angles of top surface and sidewalls. As a result, the LEE of transverse-magnetic (TM) polarized light is improved significantly. Roughening on the backside of n-AlGaN surface significantly enhances the LEE of top surface of thin-film flip-chip DUV LEDs. However, the LEE of sidewalls of thin-film flip-chip DUV LEDs is greatly weakened. For bare DUV LED, the LEE of flip-chip LED on NPSS is estimated to be about 15%, which is around 50% higher than that of thin-film flip-chip DUV LED with roughening on the backside of n-AlGaN surface.
© 2020 The Electrochemical Society ("ECS"). Published on behalf of ECS by IOP Publishing Limited. [DOI: 10.1149/2162-8777/ab85c0]

Manuscript submitted February 20, 2020; revised manuscript received March 26, 2020. Published April 9, 2020.

Group III nitride-based light-emitting diodes (LEDs) have a wide range of applications.[1–7] Among various wavelengths of LEDs, AlGaN-based deep-ultraviolet (DUV) LEDs have attracted enormous attention for their potential applications in water purification, disinfection, sterilization, biomedicine, phototherapy, and UV curing.[8–10] Owing to the significant improvement in crystal quality of AlGaN materials,[11,12] the hole injection efficiency,[13] and radiative recombination efficiency,[14,15] DUV LEDs with internal quantum efficiency above 60% have been reported.[16,17] However, the external quantum efficiency (EQE) of AlGaN-based DUV LED is still low. For device with the wavelength around 270–280 nm, the maximum EQE of DUV LEDs is reported to be about 20%,[18,19] which is much lower than that of InGaN visible LEDs.[20–23] Consequently, improving the light extraction efficiency (LEE) is considered to be critical to achieve high-performance AlGaN-based DUV LEDs.

The low LEE of AlGaN-based DUV LED is the main factor limiting the EQE. Unlike the case of visible LEDs, the low LEE of AlGaN-based DUV LED is related to (i) the high absorption of p-GaN layer to DUV photons,[24] (ii) the strong sidewall emission of AlGaN-based DUV LED.[24–26] Due to a reordering of the valence energy bands (VBs) in the high-Al-content $Al_xGa_{1-x}N$ material, the polarization of the emitted light switches from transverse-electric (TE) to transverse-magnetic (TM) mode at a threshold Al composition.[27–29] It was reported that the VB ordering in AlGaN heterostructures can be affected by the strain state and quantum confinement within the active region.[30] The electric field direction of TE polarized light is perpendicular to *c*-axis, whereas electric field direction of TM polarized light is parallel to *c*-axis. For AlGaN-based DUV LED grown on c^+(0001) sapphire substrate, TM polarized light mainly propagates in the lateral direction, resulting in a strong sidewall emission. Such an emission characteristic of AlGaN-based DUV LEDs means that technologies improving the LEE of top surface might be less effective. The structure of the LED has a significant impact on the LEE.[31–34] In the vertical LED, the LEE at the roughening top surface is enhanced while the LEE at sidewall is significantly weakened due to the removal of sapphire substrate. The recent studies show that the LEE of vertical LED with roughening on the backside of III-nitride surface is comparable to that of flip-chip LED on patterned sapphire substrate.[35,36] This phenomenon reveals that the flip-chip DUV LED on nano-patterned sapphire substrate (NPSS) could be more effective in improving the LEE than thin-film flip-chip DUV LED with roughening on the backside of n-AlGaN surface, owing to the strong sidewall emission of TM-polarized light. However, the effect of chip structure on the LEE of AlGaN-based DUV LED has not been investigated in detail.

In this study, we conducted a comparative investigation on the LEE of typical structures AlGaN-based DUV LEDs using finite-difference time-domain (FDTD) method. The LEE of the three cases of DUV LEDs were analyzed, including flip-chip DUV LED on flat sapphire substrate (FSS), flip-chip DUV LED on NPSS, and thin-film flip-chip DUV LED with roughening on the backside of n-AlGaN surface. To investigate the LEE of flip-chip devices, we first discussed the modeling method that is applicable to DUV LEDs. Then the LEE of bare DUV LEDs for each polarization mode was calculated. The effect of NPSS on the LEE of DUV LEDs was analyzed in detail. Finally, the LEEs of flip-chip DUV LED and thin-film flip-chip DUV LED were compared.

Methods

Figure 1 shows the simulation models of DUV LED on FSS, DUV LED on NPSS, and DUV LED with roughening on the backside of n-AlGaN surface. The DUV LED on FSS, DUV LED on NPSS, and DUV LED with roughening on the backside of n-AlGaN surface were denoted as DUV LED-I, DUV LED-II, and DUV LED-III, respectively. The structure parameters for the simulated flip-chip DUV LEDs were presented in Table I. The layer structure of the simulated DUV LEDs is similar to that of the reported DUV LEDs.[19] For DUV LED-III, the sapphire substrate was removed and the thickness of n-AlGaN layer was reduced to be 3 μm, while the other layers are similar to flip-chip structure. For simplicity, the effects of the electrodes, area of active layer and current spreading on LEE were not considered. These simulated DUV LEDs were embedded into a cuboid simulation domain that is terminated with a perfectly matched layer (PML). The monitors were placed at a distance of 350 nm away from the simulation model. TE and TM polarized dipoles with wavelength of 280 nm were placed in the middle plane of the AlGaN quantum-well at interval of 500 nm. The thickness and lateral dimension of sapphire substrate were set to be T and L, as shown in Fig. 1. It is indicated in Fig. 1b that the thickness of sapphire substrate did not include the height of cone-shaped pattern arrays, and the aspect ratio (R_{AR}) of sapphire substrate is defined to be T/L. For cones on sapphire substrate, the height, top diameter and interval of the patterns are 0.5 μm, 0.7 μm, and 0.3 μm, respectively. For DUV LED-III, the backside of n-AlGaN surface is roughened with cones, as shown in Fig. 1c. In DUV LED-III, the height of the cones is set to be 0.5 μm, and the bottom diameter of cones is varied from 0.5 μm to 1 μm.

[z]E-mail: zhousj@whu.edu.cn

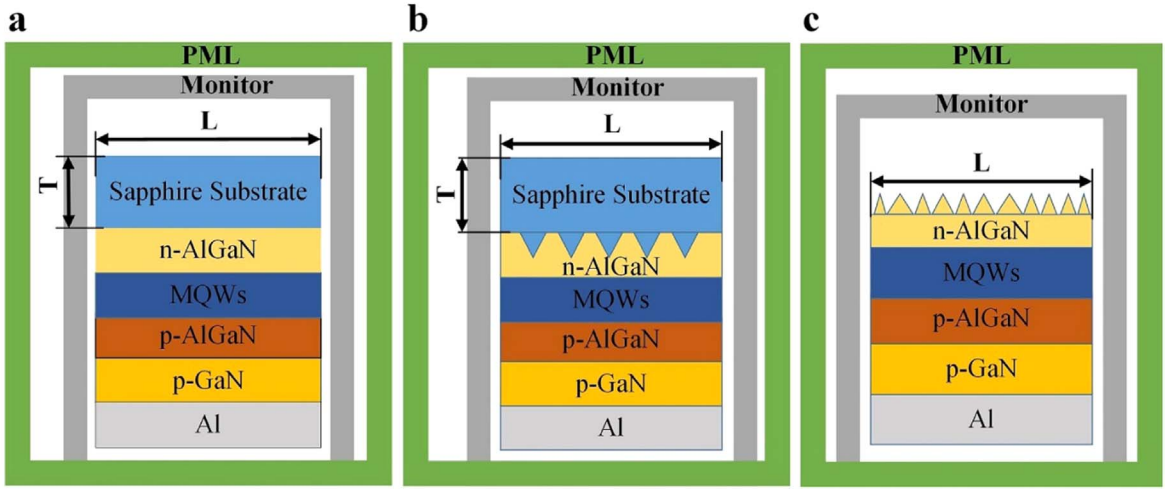

Figure 1. Simulation model of (a) flip-chip DUV LED on FSS (DUV LED-I), (b) flip-chip DUV LED on NPSS (DUV LED-II), and (c) thin-film flip-chip DUV LED with roughening on the backside of n-AlGaN surface (DUV LED-III).

Table I. Parameters for each layer used in the FDTD simulations.

Layer	Thickness (μm)	Refractive index	Absorption coefficient (cm^{-1})
p-GaN	0.1	2.5	170000
p-AlGaN	0.05	2.4	10
Quantum well	0.05	2.45	1000
n-AlGaN	3.5	2.4	10
sapphire	0-9	1.8	0

To evaluate the LEE of AlGaN-based DUV LEDs, the simulation model should be consistent with the actual DUV LED structure. However, a simplified model modeling is necessary for the simulation in the three-dimension FDTD simulation due to the limited computational memory.[37] For this objective, two kinds of modeling methods are widely used to evaluate the LEE of LED. One is to use the perfect mirror layer as the simulation boundary at the sidewall of LED,[38,39] and the other is to use a simulation model in which the R_{AR} of the sapphire substrate is consistent with the R_{AR} of the actual LED.[37] Since AlGaN-based DUV LEDs have strong sidewall emission, it is more reasonable to evaluate their LEE using the model that considers the LEE at sidewalls. Figure 2 shows the simulated LEE of DUV LED-I using a sapphire substrate with R_{AR} of 0.2. The lateral dimension of the DUV LED-I was increased from 5 μm to 25 μm, and the thickness of the sapphire substrate was increased from 1 μm to 5 μm to maintain the R_{AR} of 0.2. As the lateral dimension and thickness of sapphire substrate increased, the LEEs for both TE and TM polarized light decreased slightly, and then stabilized at approximately 7.5% and 3%, respectively. These simulation results indicated that the LEE of AlGaN-based DUV LED can be estimated using a scaled down model whose sapphire substrate has the same R_{AR} as the actual DUV LED structure. In addition, the lateral dimension should be larger than 10 μm to make the simulation results more accurate.

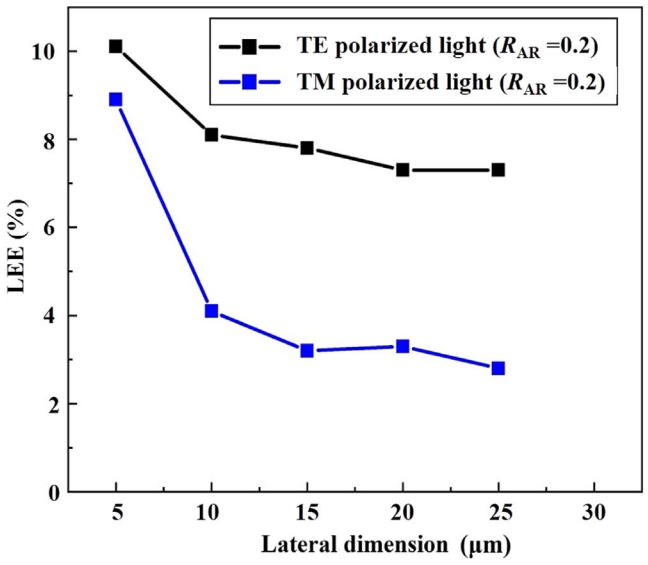

Figure 2. The simulated LEE of DUV LED-I at different lateral dimensions. The R_{AR} of sapphire substrate of DUV LED-I was maintained at 0.2.

Results and Discussion

To estimate the LEE of flip-chip DUV LED, the lateral dimension of the simulation model was kept at 12.5 μm, and the thickness of sapphire substrate was increased to extend the R_{AR} of sapphire substrate. Figure 3a shows the simulation results for TE polarized light. As the R_{AR} of sapphire substrate was extended from 0 to 0.3, the LEEs of DUV LED-I and DUV LED-II were improved significantly. When the R_{AR} was larger than 0.3, the LEE of DUV LED-I and DUV LED-II were stabilized at 8.5% and 15.1%, respectively, and a further increase in R_{AR} of sapphire substrate cannot improve the LEE of TE polarized light. In the case of $R_{AR} >$ 0.3, the LEE of DUV LED-II for TE polarized light was improved by 78% as compared to DUV LED-I. Figure 3b illustrates the simulated LEE of TM polarized light. As the R_{AR} of sapphire substrate increased from 0 to 0.75, the LEEs of DUV LED-I and DUV LED-II were enhanced, and then stabilized at 4% and 15%, respectively. When R_{AR} of sapphire substrate was set to be 0, the LEE of DUV LED-II was enhanced by 358% as compared to DUV LED-I. However, when the R_{AR} was increased from 0 to 0.4, the LEE of DUV LED-II was improved by 27%. This result indicated that the enhanced LEE for TM polarized light strongly depended on

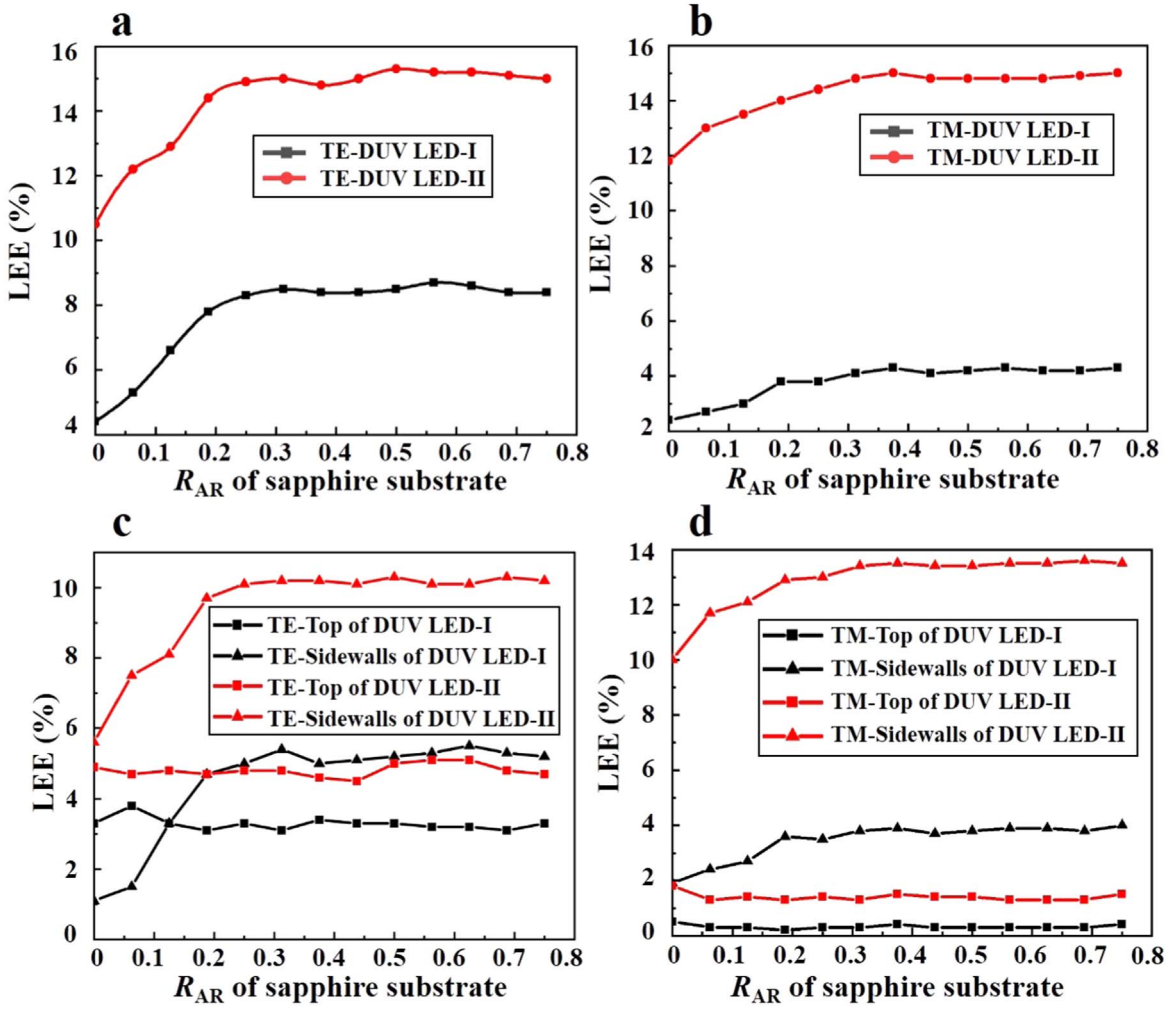

Figure 3. lEEs of DUV LED-I and DUV LED-II for (a) TE and (b) TM polarized light as a function of the R_{AR} of sapphire substrate. LEEs at top surface and sidewalls as a function of R_{AR} for (c) TE and (d) TM polarized light.

the nano-patterns of sapphire substrate rather than the increased R_{AR} of sapphire substrate. For LEDs with chip area of 300 × 300 μm^2, their R_{AR} varies from 0.3 to 0.5.[37] Consequently, the LEE of the AlGaN-based DUV LED cannot be enhanced by further increasing the R_{AR} of sapphire substrate if the R_{AR} of sapphire substrate is larger than 0.4. A similar experimental result was reported by Lee et al.[40]

To further analyze the influence of NPSS on LEE of DUV LED, the LEEs of top surface and sidewalls were separately calculated. The chip area was maintained at 12.5 × 12.5 μm^2, and the R_{AR} of sapphire substrate was increased from 0 to 0.75. Figure 3c shows the LEEs of top surface and sidewalls for TE polarized light. It was found that increasing the R_{AR} of sapphire substrate only improved the LEEs at sidewalls. Compared to DUV LED-I, the LEEs of top surface and sidewalls of DUV LED-II were improved by 50% and 409%, respectively. Figure 3d shows the simulated LEE for TM polarized light. The LEE of the top surface of DUV LEDs was almost independent on the R_{AR} of sapphire substrate, as shown in Fig. 3d. Compared to DUV LED-I, the LEE of top surface of DUV LED-II of was improved by 260% while the LEE of sidewalls of DUV LED-II was enhanced by 426%. These results showed that the NPSS technology not only improves the LEE of top surface of DUV LED, but also significantly enhances the LEE of sidewalls of DUV LED.

To understand the improvement mechanism of the LEE of AlGaN-based DUV LED, the light trajectories at AlGaN/sapphire and sapphire/air interfaces were analyzed using Snell's equation. Using the Bruggeman effective medium approximation,[41] the refractive index of cone-shaped AlGaN/sapphire medium is about 2.2. After the DUV light with a wavelength of 280 nm propagates into the cone-shaped AlGaN/sapphire medium, the light wavelength in cone-shaped AlGaN/sapphire medium is shortened to be about 130 nm, which is much smaller than the size of patterns on NPSS (700 nm). Therefore, principle of geometric optics was used to estimate the extraction angles at top surface and sidewalls of DUV LED.

According to the refractive index of AlGaN, sapphire and air, the critical angle of total internal reflection at the AlGaN/sapphire and sapphire/air interfaces are $\theta_{c1} = 48°$ and $\theta_{c2} = 34°$, respectively. The angles between the incident light rays or refracted light rays and the z-axis are θ_1 ($0° < \theta_1 < 90°$) and θ_2, respectively. Figure 4a demonstrates the typical light trajectories in DUV LED-I. Light rays refracted into FSS via flat AlGaN/sapphire interface can be divided into three parts. Firstly, refracted light rays with $\theta_2 < 34°$ can be extracted into air from the top surface. Secondly, refracted light rays with $34° < \theta_2 < 56°$ will be reflected into the AlGaN layer and lost by means of internal absorption. Thirdly, refracted light rays with $\theta_2 > 56°$ can emit into the escape cone at sidewalls, if they are incident on the sidewalls of sapphire substrate. When the incident angles are 25°, 38°, and 48°, the refraction angles at the flat AlGaN/sapphire interface are 34°, 56°, and 90°. Therefore, light rays that are incident on the flat AlGaN/sapphire interface with $\theta_1 < 25°$ can be extracted into air from the top surface, and light rays that are incident on the flat AlGaN/sapphire interface with $38° < \theta_1 < 48°$ can be extracted into air from the sidewalls of sapphire substrate.

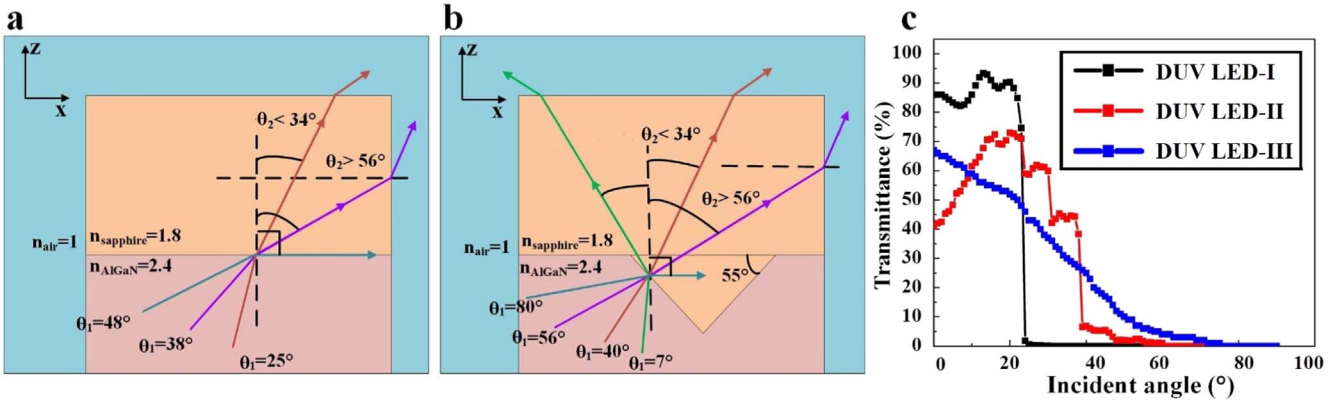

Figure 4. Typical light trajectories in (a) DUV LED-I and (b) DUV LED-II. (c) The simulated transmittance of three types of DUV LEDs as a function of incident angle.

Figure 4b demonstrates the typical light trajectories in DUV LED-II. The refracted light rays in NPSS are extracted in the same angle as the FSS, but the extraction angle of incident light changes significantly. According to height and diameter of the cone, the base angle of the cone is about 55°. When the incident angles (θ_1) of light are 56° and 80°, the corresponding refraction angles (θ_2) at cone-shaped AlGaN/sapphire interface are 56° and 90°. It is worth noting that the incident angles of $\theta_1 = 7°$ and 40° at the cone-shaped AlGaN/sapphire interface correspond to refraction angle of $\theta_2 = 34°$, as shown by the green and brown solid lines in Fig. 4b. Therefore, light rays incident on cone-shaped AlGaN/sapphire interface with angle of $7° < \theta_1 < 40°$ can be extracted into air via the top surface, while light rays incident on cone-shaped AlGaN/sapphire interface with angle of $56° < \theta_1 < 80°$ can emit into the escape cone at sidewalls of NPSS. Compared to DUV LED-I, the extraction angles at top surface and sidewalls of DUV LED-II are extended from (0°, 25°) and (38°, 48°) to (7°, 40°) and (56°, 80°) by the cone-shaped AlGaN/sapphire interface. Obviously, NPSS expands the range of extraction angles of top surface and sidewalls, which is helpful in extracting TM polarized light due to the larger incident angle of TM polarized light at AlGaN/sapphire interface.[42]

To verify the change in extraction angle at top surface, the transmittance of three types of DUV LEDs was calculated using two-dimensional FDTD simulation, as shown in Fig. 4c. A plane wave with incident angle ranging from 0° to 90° was chosen as the incident light source. Figure 4c shows the simulated transmittance of three types of DUV LEDs. For DUV LED-I, the transmittance of light rays with incident angle <25° exceeds 80%. When the incident angle is larger than 25°, the transmittance of DUV LED-I is approximately 0, indicating that the critical angle of total internal reflection in DUV LED-I was 25°. For DUV LED-II, the transmittance of light rays with incident angle <40° is larger than 40%. When the incident angle was larger than 40°, the transmittance of DUV LED-II is less than 5%. The steep drop in the transmittance of DUV LED-II at 40° indicated that there was strong total internal reflection in DUV LED-II. This phenomenon confirms the results obtained in Fig. 4b using geometrical optics. But for DUV LED-III, the transmittance decreases slowly as incident angle increases. Because the roughening AlGaN/air interface scatters light into air, the extraction angle at the top surface of DUV LED-III is significantly enlarged. These simulation results reveals that the NPSS and surface texture are more efficient to extract light rays with incident angle >25° than the FSS.

To illustrate the impact of chip structure on LEE, the LEEs of three types of DUV LEDs were calculated using FDTD method. The R_{AR} of sapphire substrate used in DUV LED-I and DUV LED-II was 0.4. Figure 5a shows the simulation results of three types of DUV LED. For both TE and TM polarized light, the LEE of DUV LED-II was the highest among these DUV LEDs, and the LEE of DUV LED-III was larger than that of DUV LED-I. Figure 5b shows LEEs of DUV LEDs at top surface and sidewalls. Among the three types of DUV LEDs, the LEE of top surface of DUV LED-III was the highest, whereas the LEE of sidewalls of DUV LED-III was the lowest. The LEEs of DUV LED-II for TE and TM polarized light are 15%. The LEEs of DUV LED-III for TE and TM polarized light are around 10%. These simulation results reveal that NPSS is a more efficient technology for improving the LEE of DUV LED than roughening on the backside of n-AlGaN surface.

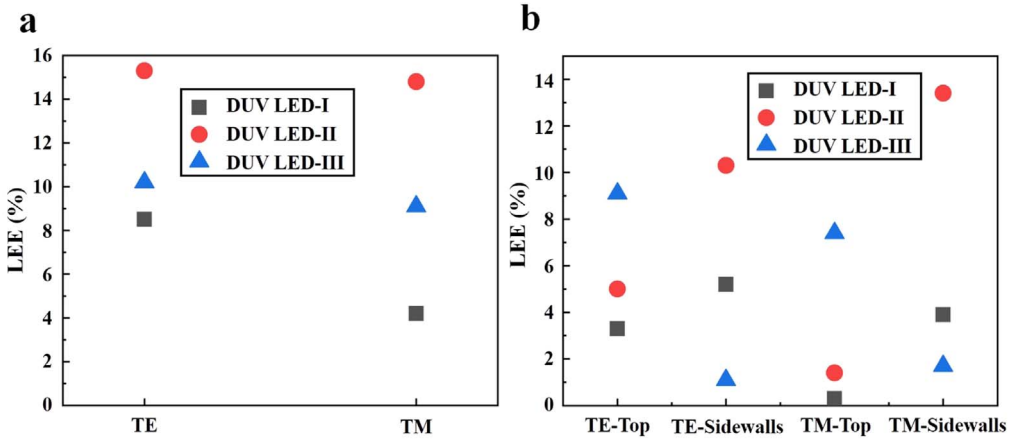

Figure 5. (a) LEEs of DUV LED-I, DUV LED-II, and DUV LED-III for TE and TM polarization light. (b) LEEs of top surface and sidewalls of DUV LED-I, DUV LED-II, and DUV LED-III.

Conclusions

In conclusion, we have applied FDTD method to analyze the effect of chip structure on LEE of AlGaN-based DUV LEDs. Compared to DUV LED on FSS, the extraction angles at top surface and sidewalls of DUV LED on NPSS are extended from (0°, 25°) and (38°, 48°) to (0°, 40°) and (56°, 80°), thereby improving the LEE of top surface and sidewalls of DUV LED. For thin-film flip-chip DUV LED with roughening on the backside of n-AlGaN surface, the LEE was enhanced at top surface but decreased at sidewalls. The NPSS extracts TM polarized light more efficiently than the roughening on the backside of n-AlGaN surface. Consequently, the NPSS is estimated to be a more efficient technology to enhance the LEE of AlGaN-based DUV LEDs than the roughening on the backside of n-AlGaN surface.

Acknowledgments

This research was funded by the National Natural Science Foundation of China (grant no. 51675386) and Natural Science Foundation of Hubei Province (No. 2018CFA091).

ORCID

Shengjun Zhou https://orcid.org/0000-0002-9004-049X

References

1. A. Khan, B. Krishnan, and K. Tom, *Nat. Photonics*, **2**, 77 (2008).
2. J. Lee, T.-Y. Seong, and H. Amano, *ECS J. Solid State Sci. Technol.*, **9**, 026005 (2020).
3. W. Guo, J. Xie, C. Akouala, S. Mita, A. Rice, J. Tweedie, I. Bryan, R. Collazo, and Z. Sitar, *J. Cryst. Growth*, **366**, 20 (2013).
4. H. Hu, B. Tang, H. Wan, H. Sun, S. Zhou, J. Dai, C. Chen, S. Liu, and L. J. Guo, *Nano Energy*, **69**, 104427 (2020).
5. C. Yan, Q. Zhao, J. Li, X. Ding, Y. Tang, and Z. Li, *Electronics*, **8**, 835 (2019).
6. M. Kneissl, T.-Y. Seong, J. Han, and H. Amano, *Nat. Photonics*, **13**, 233 (2019).
7. J. R. Grandusky, J. Chen, S. R. Gibb, M. C. Mendrick, C. G. Moe, L. Rodak, G. A. Garrett, M. Wraback, and L. J. Schowalter, *Appl. Phys. Express*, **6**, 032101 (2013).
8. S. Verma and M. Sillanpää, *Chem. Eng. J.*, **274**, 274 (2015).
9. J. Zhao, H. Hu, Y. Lei, H. Wan, L. Gong, and S. Zhou, *Nanomaterials*, **9**, 1634 (2019).
10. Y. Nagasawa and A. Hirano, *Photonics Res.*, **7**, B55 (2019).
11. H. Hirayama, Y. Tohru, N. Norimichi, O. Tomoaki, and K. Norihiko, *Appl. Phys. Lett.*, **91**, 071901 (2007).
12. P. Dong et al., *Appl. Phys. Lett.*, **102**, 241113 (2013).
13. H. X. Jiang and J. Y. Lin, *Semicond. Sci. Technol.*, **29**, 084003 (2014).
14. M. M. Satter, Z. Lochner, T. T. Kao, Y. S. Liu, X. H. Li, S. C. Shen, D. D. Russell, and P. D. Yoder, *IEEE J. Quantum Electron.*, **50**, 166 (2014).
15. Y. Zhang et al., *Superlattices Microstruct.*, **82**, 151 (2015).
16. M. Kaneda, C. Pernot, Y. Nagasawa, A. Hirano, M. Ippommatsu, Y. Honda, H. Amano, and I. Akasaki, *Jpn. J. Appl. Phys.*, **56**, 061002 (2017).
17. Z. Bryan, I. Bryan, J. Xie, S. Mita, Z. Sitar, and R. Callzao, *Appl. Phys. Lett.*, **106**, 142107 (2015).
18. T. Takano, T. Mino, J. Sakai, N. Noguchi, K. Tsubaki, and H. Hirayama, *Appl. Phys. Express*, **10**, 031002 (2017).
19. K. X. Dong, D. J. Chen, J. P. Shi, B. Liu, H. Lu, R. Zhang, and Y. D. Zheng, *Physica. E*, **75**, 52 (2016).
20. S. Zhou, H. Xu, H. Hu, C. Gui, and S. Liu, *Appl. Surf. Sci.*, **471**, 231 (2019).
21. S. Zhou, X. Liu, H. Yan, Z. Chen, Y. Liu, and S. Liu, *Opt. Express*, **27**, A669 (2019).
22. L. Tan, Q. Zhou, W. Hu, H. Wang, and R. Yao, *Appl. Sci.*, **9**, 3458 (2019).
23. B. Tang, J. Miao, Y. Liu, H. Wan, N. Li, S. Zhou, and C. Gui, *Nanomaterials*, **9**, 319 (2019).
24. J. Yun and H. Hirayama, *J. Appl. Phys.*, **121**, 013105 (2017).
25. D. Y. Kim, J. H. Park, J. W. Lee, S. Hwang, S. J. Oh, J. Kim, S. Cheolsoo, E. F. Schubert, and J. K. Kim, *Light-Sci. Appl.*, **4**, e263 (2015).
26. H. Long et al., *Phys. D-Appl. Phys.*, **49**, 415103 (2016).
27. K. B. Nam, J. Li, M. L. Nakarmi, J. Y. Lin, and H. X. Jiang, *Appl. Phys. Lett.*, **84**, 5264 (2004).
28. Y. Taniyasua and M. Kasu, *Appl. Phys. Lett.*, **96**, 221110 (2010).
29. Z. Bryan, I. Bryan, S. Mita, J. Tweedie, Z. Sitar, and R. Collazo, *Appl. Phys. Lett.*, **106**, 232101 (2015).
30. M. Lachab, W. Sun, R. Jain, A. Dobrinsky, M. Gaevski, S. Rumyantsev, M. Shur, and M. Shatalov, *Appl. Phys. Express*, **10**, 012702 (2017).
31. M. Shatalov et al., *Semicond. Sci. Technol.*, **29**, 084007 (2014).
32. C. Pernot et al., *Appl. Phys. Express*, **3**, 061004 (2010).
33. S. Zhou, X. Liu, Y. Gao, Y. Liu, M. Liu, Z. Liu, C. Gui, and S. Liu, *Opt. Express*, **25**, 26615 (2017).
34. S. Zhou, S. Wang, S. Liu, and H. Ding, *Opt. Laser Technol.*, **54**, 321 (2013).
35. Q. Zhao, J. Miao, S. Zhou, C. Gui, B. Tang, M. Liu, H. Wan, and J. Hu, *Nanomaterials*, **9**, 1178 (2019).
36. S. Zhou, H. Xu, B. Tang, Y. Liu, H. Wan, and J. Miao, *Opt. Express*, **27**, A1506 (2019).
37. T.-X. Lee, K.-F. Gao, W.-T. Chien, and C.-C. Sun, *Appl. Optics*, **52**, 1358 (2013).
38. H.-Y. Ryu, I. I.-G. Choi, H.-S. Choi, and J.-I. Shim, *Appl. Phys. Express*, **6**, 062101 (2013).
39. J. Zhao, X. Ding, J. Miao, J. Hu, H. Wan, and S. Zhou, *Nanomaterials*, **9**, 203 (2019).
40. K. H. Lee, H. J. Park, S. H. Kim, M. Asadirad, Y.-T. Moon, J. S. Kwak, and J.-H. Ryou, *Opt. Express*, **23**, 20340 (2015).
41. D. E. Aspnes, J. B. Theeten, and F. Hottier, *Phys. Rev. B*, **20**, 3292 (1979).
42. S. Wang, J. Dai, J. Hu, S. Zhang, L. Xu, H. Long, J. Chen, Q. Wan, H.-C. Kuo, and C. Chen, *ACS Photonics*, **5**, 3534 (2018).